

# The Peak Luminosity of Type Ia Supernovae and its Implications for the Cosmic Expansion Rate

Xiao-Feng Wang, Zong-Wei Li\* and Li Chen

Department of Astronomy, Beijing Normal University, Beijing 100875

Received 2000 December 18; accepted 2001 March 13

**Abstract** Supernovae of type Ia (SNe Ia) are confirmed to be the best distance indicators to derive the cosmic expansion rate. The dispersion of their peak luminosity at optical bands ( $BVI$ ) is approximate to 0.13 mag, after taking into account the effects of the second parameters (i.e., the initial decline rate  $\Delta m_{15}(B)$  and  $(B - V)$  color at maximum light). The local calibrations from HST indicate an absolute magnitude of  $19.48 \pm 0.08$  mag (in  $V$  band) for SNe Ia in spiral galaxies. The current expansion rate,  $H_0$ , is found to be  $63.6 \pm 1.8$  (random)  $\pm 5.7$  (systematic)  $\text{km s}^{-1} \text{Mpc}^{-1}$ . This value will decrease by 3% when the metallicity effect on the cepheid distances is considered. In addition, a marginal local outward flow of  $4.0 \pm 4.5\%$  within the velocity-distance of  $7\,000 \text{ km s}^{-1}$  can be inferred from SNe Ia for the Einstein-de Sitter universe; however, this outward flow is only  $2.2 \pm 4.4\%$  for an accelerating expansion universe (which is supported by high- $z$  SNe Ia).

**Key words:** Cosmology: observations – distance scale – supernovae: general

## 1 INTRODUCTION

Interest in type Ia supernovae (SNe Ia) has risen dramatically with their application to the cosmological problems since Kowal (1968). Their powerful capabilities as distance indicators on the cosmic scale have pushed them into the limelight of cosmology. They now provide the main route to the current expansion rate and the deceleration of the universe. (see Branch 1998; Perlmutter et al. 1999; Riess et al. 1998).

SNe Ia are universally accepted as the result of thermonuclear explosion of accreting C+O white dwarfs in binary systems. They reach a luminosity of the same order as that of their host galaxies, a million times greater than cepheids. The photons SNe Ia emitted at more than half of the age of the universe could still be detected. Moreover, they are easier to understand than their parent galaxies because the evolution for the explosion of a single object would be less dependent on different distance scales. Therefore, SNe Ia are considered to be better standard candles on the cosmic scale.

In the past decade, both observational data and theoretical investigations have shown that SNe Ia are not standard candles of constant peak luminosity as we had believed. The variation

---

\* E-mail: lizw@bnu.edu.cn

in the peak luminosity is  $\sim 3$  mag in  $B$  and  $\sim 2$  mag in  $V$ , which is probably an indication of different progenitor populations; a variation of this size challenges their role as standard candles. Branch et al. (1993) pointed out that SNe Ia can be classified into normal (now called Branch normal) and peculiar ones, according to their spectrum behavior. It has been shown that just excluding the spectroscopically peculiar events, or by selecting those with  $B - V$  at maximum smaller than 0.25 mag (see Vaughan et al. 1995), reduces the scatter in the Hubble diagram to values around  $\sigma \sim 0.25$  mag (Hamuy et al. 1996a). More fortuitously, a strong correlation between the peak luminosity and the initial decline rate of the light curve was found. Phillips (1993) introduced  $\Delta m_{15}(B)$ , defined by the decline in magnitudes during the first 15 days after  $B$  maximum, as a measure of the decline rate. Other ways to describe the shape of the light curve are given in Riess et al. (1995) and Perlmutter et al. (1997).  $B - V$  color of SNe Ia at maximum has been frequently suggested to be another important second parameter influencing the intrinsic peak luminosity (see Tripp & Branch 1999, Parodi et al. 2000). The scatter in the Hubble diagram will be further reduced to  $\sim 0.13$  mag using the second parameters to standardize the peak luminosity.

In this paper, we use spectroscopically normal SNe Ia suffering negligible reddening in their parent galaxies (called blue SNe Ia) to re-analyze the relations between the peak luminosity and the second parameters. The relations are then used to correct the peak luminosity of the Hubble-flow SNe Ia and the cepheid-based calibrators in nearby galaxies, and hence to derive the expansion rate,  $H_0$  and its possible variations with distances. We present the peak luminosity calibration of SNe Ia from HST in Section 2, and the Hubble diagram in Section 3. In Section 4, we re-examine the correlations of the peak luminosity with the second parameters. We show the results of  $H_0$  in Section 5. In Section 6, we briefly discuss the variations of the expansion rate  $H_0$  with distances inferred from SNe Ia, and in Section 7, we summarize our conclusions.

## 2 THE ABSOLUTE MAGNITUDE CALIBRATIONS OF SNe Ia

The premise to determine the expansion rate by SNe Ia is to know their absolute magnitudes, which need to be calibrated by other means. At present, through their Period-Luminosity (PL) relation, the cepheids are the most reliable and least controversial distance indicators. Due to their low luminosity, however, even with the Hubble Space Telescope (HST), it is not possible to study cepheids out to distances at which random motions of galaxies are negligible compared to the cosmic Hubble flow. Nevertheless, it might be possible to use cepheids to calibrate the absolute magnitudes of SNe Ia occurring in nearby galaxies. To date, HST has provided direct cepheid distances to nine galaxies which have produced 10 SNe Ia. The spectroscopically peculiar SN 1991T in NGC 4527 and the oldest, SN 1895B, observed photographically in only one color are not used here. This leaves eight galaxies with eight SNe Ia. They are listed in Table 1, which has the following format:

Columns (1),(2): SN name, and the name of the host galaxy. Columns (3),(4),(5): The apparent  $BVI$  peak magnitudes of SNe Ia. Column (6): References to the SN photometry. Columns (7),(8): The reddening  $E(B - V)$  and their references. Columns (9),(10): The true distance moduli of the host galaxy derived by Saha and Gibson respectively. Columns (11),(12): The observed value of the decline rate parameter  $\Delta m_{15}(B)$ (see Column (6) for references), and the observed  $B - V$  color at maximum light.

**Table 1** The Absolute Magnitudes of SNe Ia in  $B$ ,  $V$  and  $I$  Calibrated Through Cepheid Distances to Their Parent Galaxies

(1)	(2)	(3)	(4)	(5)	(6)	(7)	(8)	(9)	(10)	(11)	(12)
SN	Host Galaxy	$B_{\max}$	$V_{\max}$	$I_{\max}$	ref.	$E(B - V)$	ref.	$(m - M)_0^a$	$(m - M)_0^b$	$\Delta m_{15}$	$B_{\max} - V_{\max}$
1937C	IC 4182	8.82(12)	8.86(13)	...	1,2,3	0.017(002)	11	27.92(07)	27.61(11)	0.93(13)	-0.07
1960F	NGC 4496A	11.60(12)	11.51(18)	...	4,5	0.025(002)	11	31.03(14)	31.02(07)	1.06(12)	0.06
1972E	NGC 5253	8.49(14)	8.49(15)	8.80(19)	3	0.056(006)	11	28.31(07)	28.31(11)	0.87(10)	-0.06
1974G	NGC 4414	12.48(05)	12.30(05)	...	6	0.16(07)	6	31.41(17)	31.41(10)	1.11(06)	0.02
1981B	NGC 4536	12.03(03)	11.93(03)	...	3	0.10(03)	5	31.10(13)	30.95(07)	1.10(05)	0.00
1989B	NGC 3627	12.34(05)	12.02(05)	11.75(05)	7	0.37(03)	7	30.22(12)	30.06(17)	1.31(07)	-0.05
1990N	NGC 4639	12.76(03)	12.70(02)	12.94(02)	8	0.026(003)	11	32.03(22)	31.80(09)	1.03(06)	0.04
1998bu	NGC 3368	12.21(03)	11.88(03)	11.67(05)	9,10	0.365(06)	9,10	30.37(16)	30.20(10)	1.01(05)	-0.04

References: (1) Pirece& Jacoby 1995; (2) Schaefer 1996; (3) Hamuy et al. 1996; (4) Schaefer 1996; (5) Saha et al. 1996b; (6) Schaefer 1998; (7) Wells et al. 1994; (8) Lira et al. 1998; (9) Suntzeff et al. 1999; (10) Jha 1999; (11) Schlegel et al. 1998.

<sup>a</sup> The true distance modulus derived by Saha et al. (1994 for IC 4182, 1995 for NGC 5253, 1996a for NGC 4536, 1996b for NGC 4496A, 1997 for NGC 4639, 1999 for NGC 3627) but for NGC 4414 (Turner et al. 1998) and NGC 3368 (Tanvir et al. 1995).

<sup>b</sup> The true distance modulus re-analyzed by Gibson et al. 2000.

Note. The true distance modulus of IC 4182 and NGC 4496A in Column(9) have been corrected for "long" exposure zero-point (see Gibson et al. 2000).

The reddenings of SNe 1937C, 1960F, 1972E listed in column (7) only include the Galactic part. However, evidence from many directions shows that the extinctions they suffer in their parent galaxies are likely to be quite low (Branch 1998). The absolute  $BVI$  peak magnitudes of SNe Ia can be calculated from their apparent magnitudes, the true distance modulus of the host galaxy, and the reddening. As may be seen from Table 1, the true distance moduli re-analyzed by Gibson et al. (2000) are 0.12 mag smaller on average than those obtained by Saha et al. (1994, 1995, 1996a, 1996b, 1997, 1999), leading to a systematic discrepancy of the deduced mean absolute magnitudes by almost the same amount. These two sets of distance moduli are derived by the same HST archives, and based on the same zero-point of  $(m - M)_{\text{LMC}} = 18.50$ . The main difference lies in the procedure of photometry (DoPHOT vs. ALLFRAME) and the associated method of detecting variable stars. We do not want to over-interpret the available data here (see Saha et al. 2000; Gibson et al. 2000 for details).

A simple weighted average of these two sets of absolute magnitudes would be inappropriate, for some of the deduced values are incompatible within their error bars. As an alternative, we use the Bayesian approach (Press 1997) to derive the probability distribution of the SNe Ia absolute magnitudes based on these two distance modulus sets. Figure 1 shows the probability distribution of the absolute magnitudes in  $B$ ,  $V$  and  $I$ . At the level of 68.3% they are given as

$$M_B = -19.50 \pm 0.08, \quad (1)$$

$$M_V = -19.48 \pm 0.08, \quad (2)$$

$$M_I = -19.16 \pm 0.12. \quad (3)$$

These results are in agreement with the explosion models, ejecting about  $0.6M_{\odot}$  of  $^{56}\text{Ni}$ , by Hoflich & Khokhlov (1996) for SNe Ia with equal decline rate and blue color.

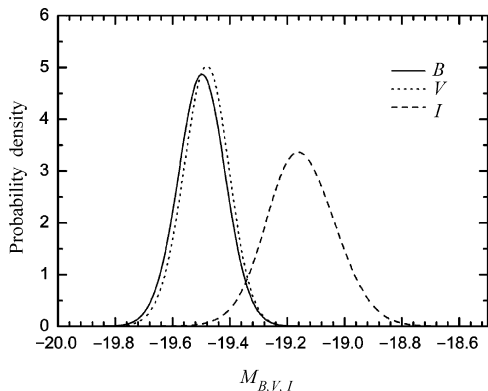


Fig. 1 The relative probability distribution of the absolute magnitudes by Bayesian approach for eight SNe Ia of Table 1

Direct cepheid distances to SNe Ia in galaxies of early Hubble types are unavailable until now, since it is difficult to find young variable stars in E/S0 galaxies. The distances to SNe 1980N, 1981D in NGC 1316, SN 1992A in NGC 1380, SN 1994D in NGC 4526 have been derived by means of globular clusters (Richtler & Drenkhahn 1999). These distances led to lower absolute magnitudes of SNe Ia. However, Blakeslee et al. (1996) found evidence that the turn-over magnitudes (TOM) of globular clusters may depend on environment: TOM decreasing with increasing local density. Such an effect makes the GCLF (globular cluster luminosity function) less useful for determining distances. The indirect cepheid distances to SNe Ia in early type galaxies inferred from spiral members are rather uncertain because of the depth effect of the galaxy cluster.

### 3 THE HUBBLE DIAGRAM

The fiducial sample used to construct the Hubble diagram contains 35 blue SNe Ia discovered after 1985 and with  $1400 \leq v \leq 37500 \text{ km s}^{-1}$ . They are confirmed to be spectroscopically normal and to suffer negligible reddening in their parent galaxies (see Parodi et al. 2000). These SNe Ia are not so remote ( $z < 0.12$ ); however, the still uncertain value of  $q_0$  would lead to some uncertainty. We use the equation below to describe the  $m - z$  relation:

$$m = 5 \log cz + 5 \log \left( 1 + \frac{(1 - q_0)z}{2} \right) + M - 5 \log H_0 + 25, \quad (4)$$

which is valid for all models.  $m$  is the observed apparent magnitudes at maximum light, corrected for Galactic extinction (Schlegel et al. 1998) and the  $K$  terms (Hamuy 1993) whenever possible, and  $z$  is the measured redshift.  $M$  is the absolute magnitudes of SNe Ia at maximum light. According to the evidence of Riess et al. (1998) and Perlmutter et al. (1999) for an accelerating expansion universe, we fix the value of  $q_0$  at  $-0.55$ . A negative  $q_0$  is also supported by the not-so-distant fiducial sample for a tighter Hubble relation compared to other values. As proposed by Tammann et al. (2000), it is possible to obtain significant values of  $(\Omega_M, \Omega_\Lambda)$  from 100 – 200 SNe Ia with  $z < 0.12$  with good observations.

The Hubble diagrams in  $B$ ,  $V$  and  $I$  of the 35 SNe Ia of the fiducial sample are shown in Figure 2. The overall rms scatter in apparent magnitudes is 0.225 mag in  $B$ , 0.201 mag in  $V$ , and 0.182 mag in  $I$ , confirming SNe Ia at maximum light to be powerful distance indicators. However, inspection of Figure 2 reveals two effects: 1) SNe Ia in spirals are  $0.19 \pm 0.08$  mag brighter in  $B$ ,  $0.16 \pm 0.07$  mag brighter in  $V$ , and  $0.16 \pm 0.06$  mag brighter in  $I$  than those in E/S0 galaxies. 2) Distant SNe Ia ( $3.8 < \log cz < 4.6$ ) are fainter than nearer ones ( $3.1 < \log cz < 3.8$ ) by  $0.15 \pm 0.10$  mag in  $B$ ,  $0.13 \pm 0.10$  mag in  $V$  and  $0.09 \pm 0.08$  mag in  $I$ . These two apparent effects can naturally be solved when the effect of the second parameters is considered in the next section.

#### 4 DEPENDENCE OF THE SNe Ia PEAK LUMINOSITY ON THE SECOND PARAMETERS

The rms scatter in apparent magnitudes around the Hubble diagram in Figure 2 can be reduced further, for the variation of the peak luminosity is not erratic but shows a systematic behavior. As suggested earlier by some authors and quantified by Phillips (1993), the peak luminosity of SNe Ia shows a strong correlation with the initial decline rate,  $\Delta m_{15}(B)$ : the more luminous the SNe Ia is, the slower its light curves decline; and vice versa. Hamuy et al. (1996a) confirmed the correlation but for a much flatter slope. The peak luminosity also correlates with the parent-galaxy type (Hamuy et al. 1996b) and with the parent-galaxy color (Branch et al. 1996). The galaxies of late Hubble types (bluer colors) tend to host more luminous SNe Ia. In fact, both the  $B - V$  colors and the type of the parent galaxies correlate with the decline rate,  $\Delta m_{15}(B)$  (see figure 2 in Branch et al. 1996, and figure 6 in Hamuy et al. 1996b). Wang et al. (1997) claimed that the luminosity scatter tends to be smaller with increasing galactocentric distance. In recent years, the  $B - V$  color of SNe Ia at maximum light (hereafter  $B_{\max} - V_{\max}$ ) have frequently been suggested to be an important independent second parameter influencing the peak luminosity (see Tripp & Branch 1999, Parodi et al. 2000), bluer SNe Ia being brighter. In order to examine which parameters among those parameters mentioned above are important, we made a gradual regression analysis by considering the peak luminosity of SNe Ia as a linear function of those parameters. The  $F$  test shows that  $\Delta m_{15}(B)$  and  $(B_{\max} - V_{\max})$  are the most important parameters accounting for the variation of the peak luminosity at the level of 95%. The solutions of the linear regression are :

$$\delta M_B = 0.60 (0.10) (\Delta m_{15}(B) - 1.2) + 1.97 (0.44) (B_{\max} - V_{\max} + 0.01) , \quad (5)$$

$$\delta M_V = 0.60 (0.10) (\Delta m_{15}(B) - 1.2) + 0.97 (0.44) (B_{\max} - V_{\max} + 0.01) , \quad (6)$$

$$\delta M_I = 0.52 (0.10) (\Delta m_{15}(B) - 1.2) + 0.64 (0.42) (B_{\max} - V_{\max} + 0.01) . \quad (7)$$

The first and second terms on the right of these equations correct the observed peak luminosity of each SN to the equivalent peak luminosity of an event with  $\Delta m_{15}(B) = 1.2$  and  $(B_{\max} - V_{\max}) = -0.01$ . The solutions above are consistent with those got by different subsamples of SNe Ia (see Table 2).

**Table 2** The Correlation of the Peak Luminosity with  $\Delta m_{15}(B)$  and  $(B_{\max} - V_{\max})$

(1)	(2)	(3)	(4)	(5)
sample	Number	$\Delta m_{15}(B)$	$B_{\max} - V_{\max}$	$R$
All	35	0.59(0.10)	1.97(0.44)	0.83
$B$ Spirals	15	0.48(0.29)	2.18(0.87)	0.72
E/S0	20	0.58(0.16)	1.90(0.52)	0.83
All	35	0.59(0.10)	0.97(0.44)	0.78
$V$ Spirals	15	0.48(0.29)	1.18(0.87)	0.59
E/S0	20	0.58(0.16)	0.90(0.52)	0.76
All	30	0.52(0.10)	0.64(0.42)	0.75
$I$ Spirals	13	0.50(0.29)	0.29(0.87)	0.51
E/S0	17	0.47(0.14)	0.96(0.43)	0.80

Note:  $R$  represents the correlation coefficients.

To uncover the effects of the decline rate and of the color, the variation of the peak luminosity is plotted as a function of  $\Delta m_{15}(B)$  and  $(B_{\max} - V_{\max})$  in Figure 3 and Figure 4, respectively. The correlation of  $\delta M_{B,V,I}$  with  $\Delta m_{15}(B)$  is obvious in  $B$ ,

**Table 3** The Mean Decline Rate and Color of SNe Ia

Sample	Number	$\Delta m_{15}(B)$	$B_{\max} - V_{\max}$
All	35	1.236(0.041)	-0.009(0.009)
Spirals	15	1.048(0.041)	-0.005(0.013)
E/S0	20	1.377(0.044)	-0.014(0.013)
Calibrators	8	1.053(0.048)	-0.010(0.016)

$V$  and  $I$ , fast decliners being intrinsically faint. Such a behavior is also theoretically understandable. If the light curve is triggered by the decay of  $^{56}\text{Ni}$ , the available amount of Ni should have a considerable effect. The higher the Ni mass, the brighter the SN, and the longer the time needed for the deposited energy to be radiated away (Hoflich et al. 1996). Mazalli et al. (2000) explored the possibility that a series of Chandrasekhar-mass explosion models, which differ essentially in the amount of  $^{56}\text{Ni}$  they synthesize, can explain the observed range of the peak luminosity, at least for the spectroscopically normal SNe Ia. Their results are not very

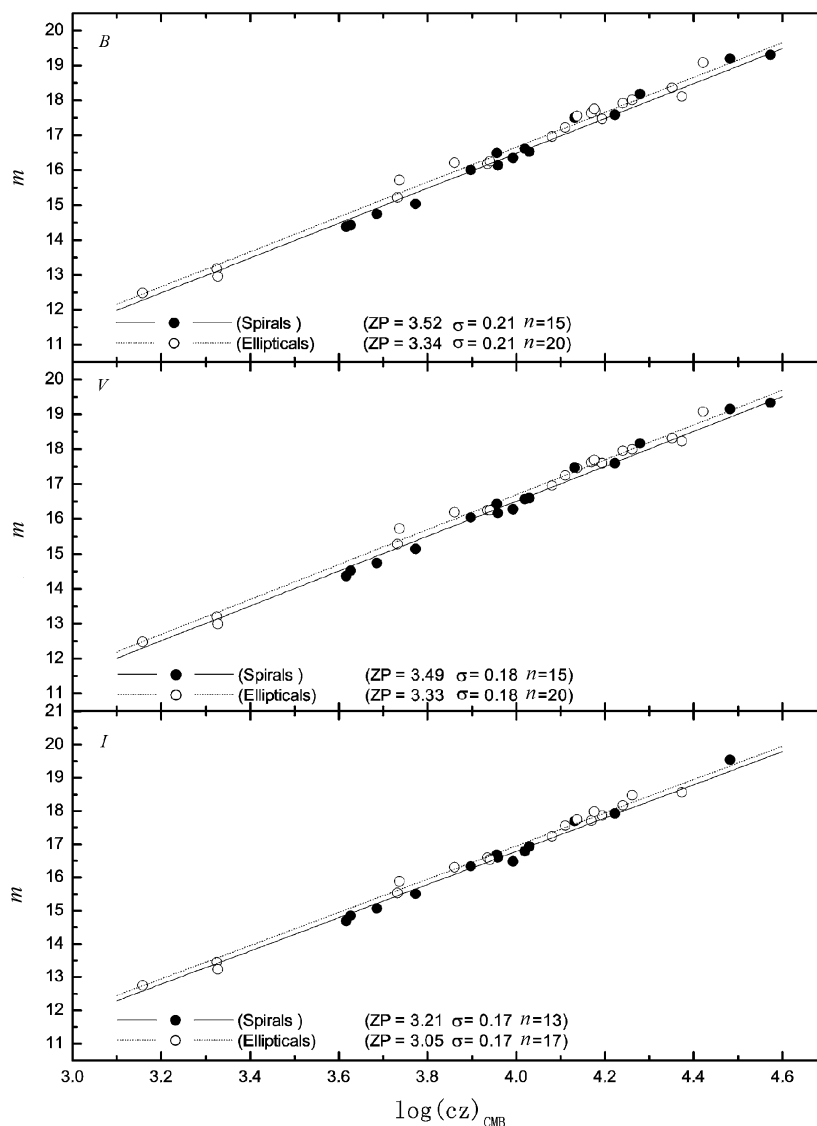


Fig. 2 The raw Hubble diagram of the 35 SNe Ia of the fiducial sample. Different symbols are used for SNe Ia in spirals and in E/S0 galaxies. The solid line is a linear fit of slope 5 to the SNe Ia in spirals; the dotted line is the corresponding fit for SNe Ia in E/S0 galaxies.

reliable, but encouraging. The observed variation in  $(B_{\max} - V_{\max})$  also account partly for the luminosity differences of SNe Ia. Eqs. (5)–(7) show that the coefficients in the color terms are much smaller than the standard extinction coefficients of 4.3 in  $B$ , 3.3 in  $V$  and 2.0 in  $I$ . Therefore, most part of the observed  $(B_{\max} - V_{\max})$  color is intrinsic to the SNe Ia rather than being due to extinction. Another strong proof comes from the observation that the coefficients of the color terms defined by SNe Ia in spirals alone are similar to those in E/S0 (less gas and

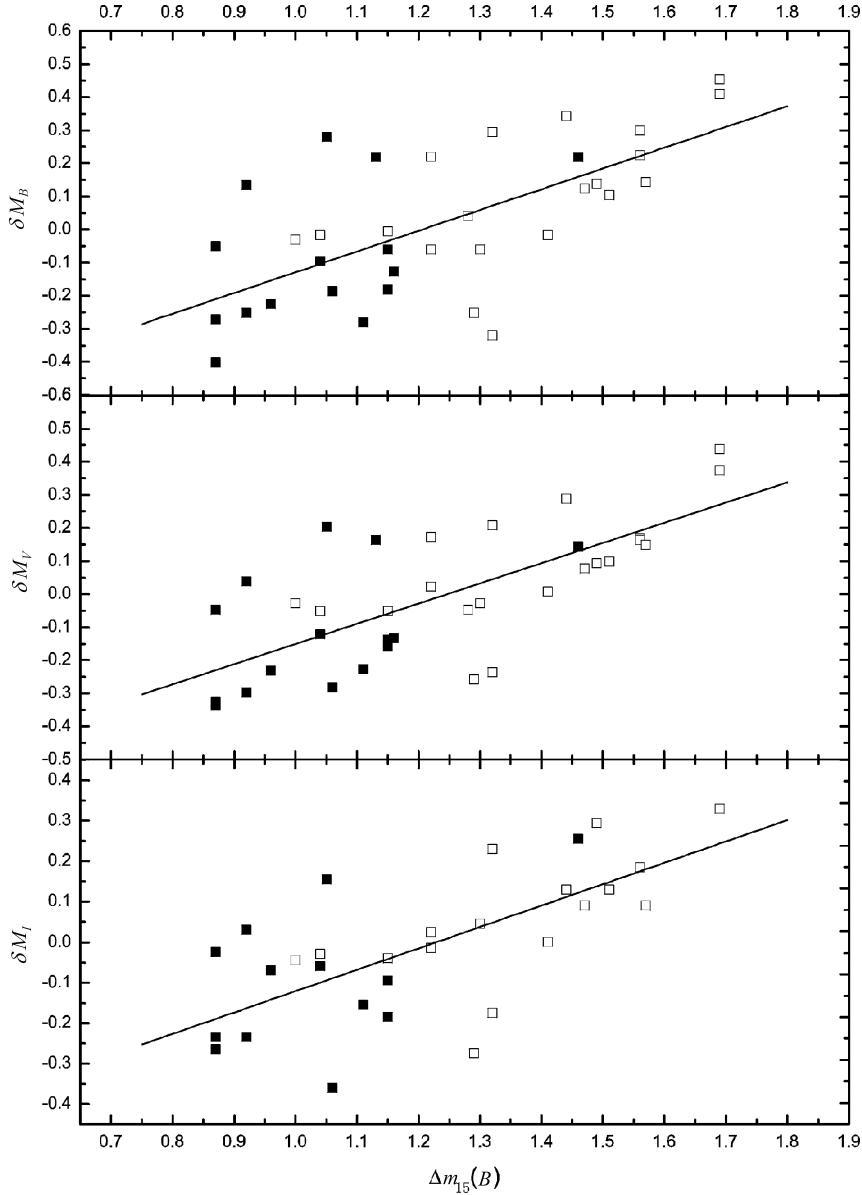


Fig. 3 The variations of the peak luminosities (i.e., residuals from the Hubble line in Fig. 2) for the SNe Ia of the fiducial sample as a function of the decline rate  $\Delta m_{15}(B)$ . Filled symbols represent SNe Ia in spirals; open symbols are those in E/S0 galaxies.

dust). Colors are the indication of the photosphere temperature. Khokhlov et al. (1993) pointed out that the temperature may have a significant influence on the opacity, which is a key factor affecting the efficiency of energy transport. Consequently, it is not difficult to understand the correlation between the variations of the peak luminosity and the colors in Figure 4.

If the apparent magnitudes  $m_{B,V,I}$  of the fiducial sample are corrected for  $\Delta m_{15}(B)$  and  $(B_{\max} - V_{\max})$  by means of Eqs. (5)–(7), the scatter in apparent magnitudes in Figure 2 will

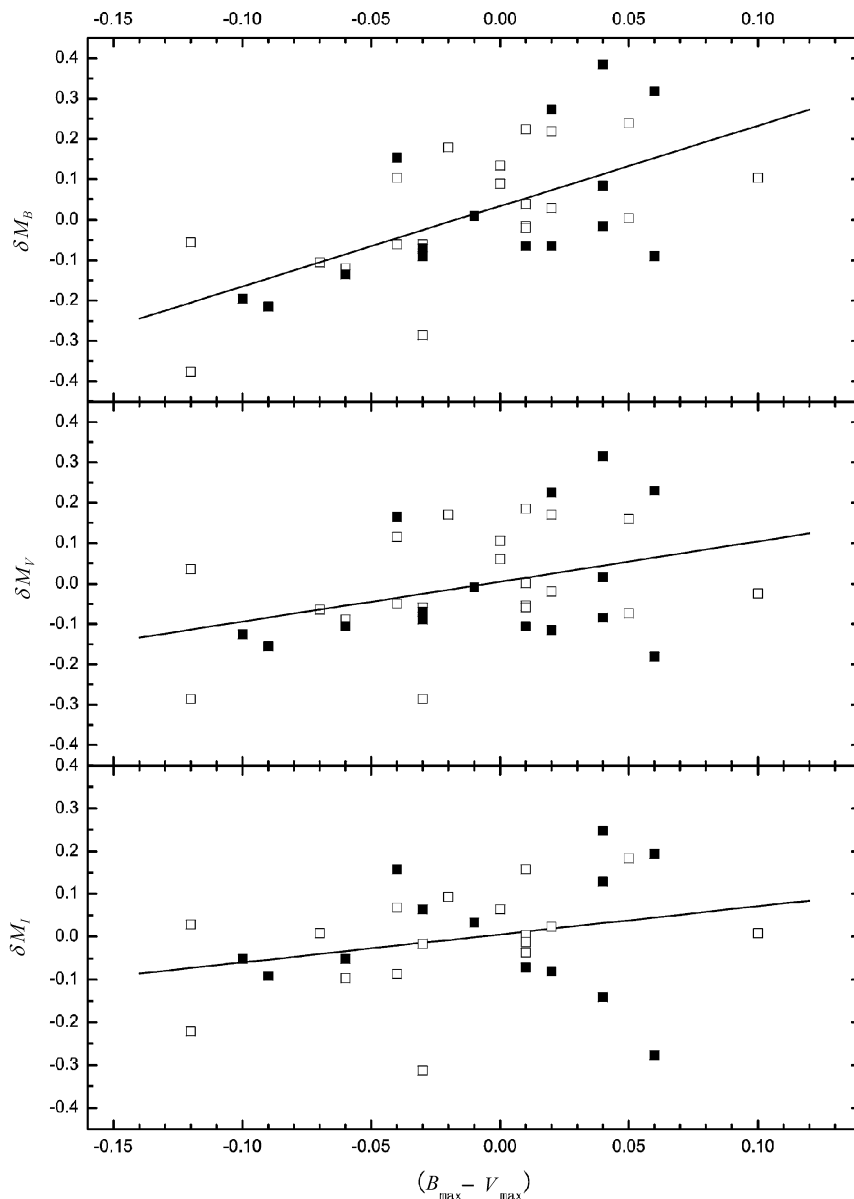


Fig. 4 The variations of the peak luminosities (i.e., residuals from the Hubble line in Fig. 2) for the SNe Ia of the fiducial sample as a function of the color  $(B_{\max} - V_{\max})$ . The symbols are the same as those in Figure 3.

decrease to 0.133 mag in  $B$ , 0.133 mag in  $V$  and 0.133 mag in  $I$  (see Figure 5). Here the small rms scatter might be attributed as essentially due to observational errors. It is unlikely that the universe will ever offer better distance indicators than SNe Ia. As seen from Table 3, the mean color  $\langle B_{\max} - V_{\max} \rangle$  of SNe Ia in spirals is only  $0.007 \pm 0.018$  mag redder than those in E/S0 galaxies, while their mean decline rate  $\langle \Delta m_{15}(B) \rangle$  is  $0.329 \pm 0.060$  mag slower than their counterparts. Therefore, such corrections are necessary to ensure the consistency of the overall sample being used to derive the Hubble constant. The systematic luminosity difference between

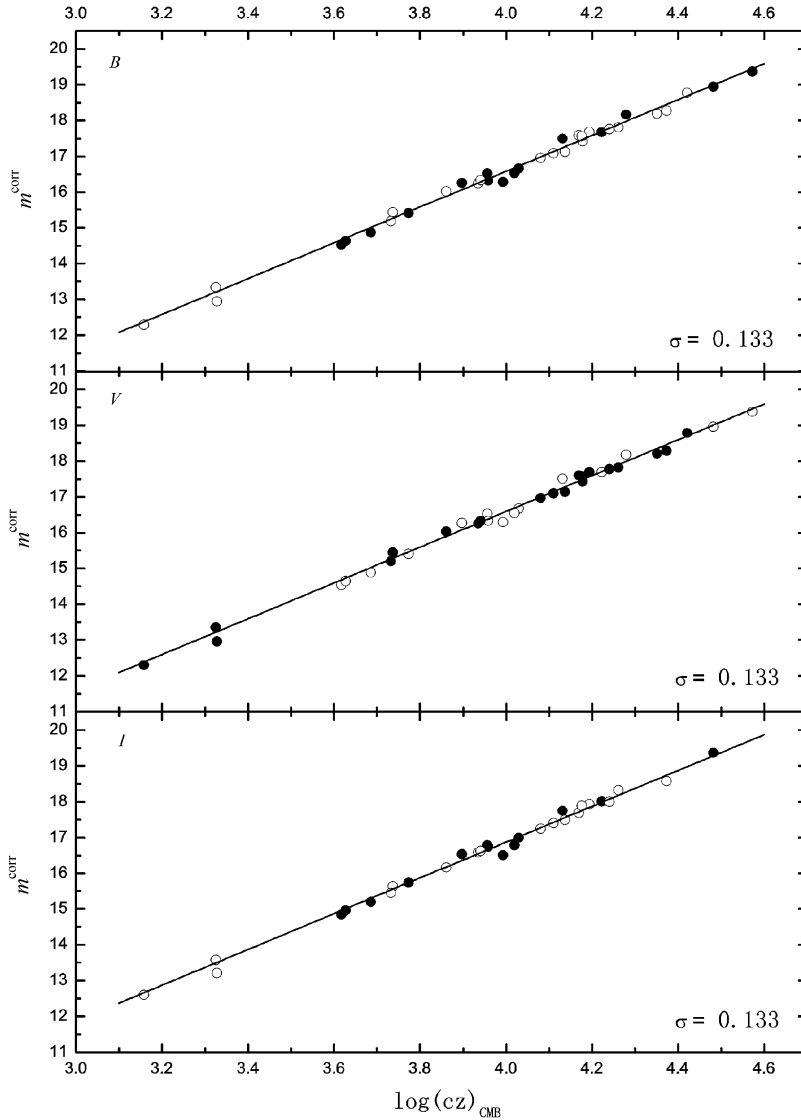


Fig. 5 The Hubble diagram of the fiducial sample after corrections for  $\Delta m_{15}(B)$  and  $(B_{\max} - V_{\max})$ . The symbols are the same with Fig. 2. Solid line is the fit of slope 5 to all SNe Ia.

SNe Ia in spirals and E/S0 galaxies shown in Figure 2 disappears after the correction for these two parameters (i.e., the zero-points of the fit of slope 5 to SNe Ia in spirals and in E/S0 differ by less than 0.01 mag). Moreover, the luminosity difference between distant SNe Ia and nearer ones now becomes marginally important.

The mean color  $\langle B_{\max} - V_{\max} \rangle$  of the eight calibrators listed in Table 1 is almost the same as that of the fiducial sample, but the mean decline rate  $\langle \Delta m_{15}(B) \rangle$  of the former is  $0.186 \pm 0.050$  mag slower than that of the latter. So the absolute magnitudes of the eight calibrators must be corrected by the same mean values. The corrected absolute magnitudes in  $B$ ,  $V$  and  $I$  are

$$M_B = -19.40 \pm 0.08, \quad (8)$$

$$M_V = -19.39 \pm 0.08, \quad (9)$$

$$M_I = -19.09 \pm 0.13. \quad (10)$$

## 5 THE HUBBLE CONSTANT

### 5.1 Deriving the Value of $H_0$

According to Eq. (4), the Hubble constant  $H_0$  can be expressed as

$$\log H_0 = 0.2(M - m) + \log(cz) + \log\left(1 + \frac{(1 - q_0)z}{2}\right) + 5. \quad (11)$$

For each supernova of the fiducial sample, we use Eq. (11) to evaluate  $H_0$  using the value of  $M_{B,V,I}$  from Eqs. (8)–(10). The uncertainty in  $H_0$  for each supernova is obtained by combining in quadrature the quoted errors in the apparent magnitudes (the errors introduced by  $\Delta m_{15}(B)$  and  $(B_{\max} - V_{\max})$  having been included), in the absolute magnitude and in the peculiar motion of the parent galaxy with respect to the Hubble flow, which is

$$\delta H_0 = H_0 \sqrt{\left(\frac{\ln 10}{5}\right)^2 [(\delta m)^2 + (\delta M)^2] + \left[\left(\frac{1}{z} + \frac{1 - q_0}{2}\right) \delta z\right]^2}. \quad (12)$$

Treating the 35 values of  $H_0 \pm \delta H_0$  in  $B$ ,  $V$  and 30 values in  $I$  by the Bayesian method led to  $H_0(B) = 63.6 \pm 1.7$ ,  $H_0(V) = 63.7 \pm 1.7$ , and  $H_0(I) = 63.6 \pm 1.8$ . The three colors  $B$ ,  $V$ , and  $I$  give closely the same result, with a mean value of

$$H_0(BVI) = 63.6 \pm 1.8 \text{ km s}^{-1} \text{ Mpc}^{-1} (1\sigma). \quad (13)$$

The errors represent only the statistical. The  $H_0$  value we obtain may still be affected by systematic errors. The important sources of systematic errors are:

1) The zero point of the cepheid PL relation is still controversial. Many researches in the last one or two years (Feast 1999; Walker 1999; Ferderspiel et al. 1998) suggested that the adopted zero-point  $(m - M)_{\text{LMC}} = 18.50$  (Madore & Freedman 1991) is likely to be too small by 0.06 mag. Hipparcos data seem to give an even higher zero-point. However, both the luminosity of the red clump and eclipsing binaries support  $(m - M)_{\text{LMC}} < 18.50$ . Recently, Freedman et al. (2001) demonstrated that a downward revision of 0.05 mag is appropriate. Conservatively speaking, an uncertainty of 0.10 mag in the LMC zero-point does exist.

2) To date, no agreement has been reached as to the cepheid distance  $(m - M)_0$  as a function of cepheid metallicity  $[O/H]$  (or  $[Fe/H]$ ). Theoretical investigations seem to demonstrate that

metallicity dependence of the PL relations is nearly negligible (Alibert et al. 1999; Sandage et al. 1999). The sign of empirical corrections is also puzzling. Some estimates that apply to cepheid distances derived from  $V$  and  $I$  observations are  $\delta(m - M)_0/\delta [\text{O}/\text{H}] \sim -0.4 \text{ mag dex}^{-1}$  (Sasselov et al. 1997; Beaulieu et al. 1997), and  $\sim -0.24 \text{ mag dex}^{-1}$  (Kennicutt et al., 1998) which increasing the distance of galaxies more metal rich than the LMC. On the other hand, Bono et al. (1999) derived  $\delta(m - M)_0/\delta [\text{O}/\text{H}] \sim 0.75 \text{ mag dex}^{-1}$ , which acts in the opposite direction, decreasing the distance to galaxies more metal rich than the LMC. Based on the cepheid field metallicities listed in Gibson et al. (2000), an uncertainty of 0.08 mag should be assigned to the derived cepheid modulus.

3) Other large systematic errors are involved with the stellar profile crowding on WFPC2 and the calibration zero-point of WFPC2 of HST. They are estimated to be  $\pm 0.10 \text{ mag}$  and  $\pm 0.07 \text{ mag}$  respectively, after Freedman et al. (2001).

In combination, the above systematic error (amounting to 0.18 mag in total) yields a final result for the Hubble constant of

$$H_0 (BVI) = 63.6 \pm 1.8 \pm 5.7 \text{ km s}^{-1} \text{ Mpc}^{-1} (1\sigma). \quad (14)$$

Considering the metallicity dependency in the cepheid  $PL$  relation (i.e., using  $(m - M)_0/\delta [\text{O}/\text{H}] \sim -0.2 \pm 0.2 \text{ mag dex}^{-1}$ ) will decrease  $H_0$  by  $1.8 \text{ km s}^{-1} \text{ Mpc}^{-1}$ . If  $q_0$  is assumed to be 0.50, the value of  $H_0$  will decrease by  $1.2 \text{ km s}^{-1} \text{ Mpc}^{-1}$ . The  $H_0$  value in Eq. (14) will be underestimated by 6% without corrections for the decline rate and the color.

## 5.2 Comparison with Other Results

We compared our results of  $H_0$  with those given in recent literature. The objective value of  $H_0$  obtained by Parodi et al. (2000) is  $60.9 \pm 2.0 (\text{random}) \text{ km s}^{-1} \text{ Mpc}^{-1}$ . The cepheid distances Parodi et al. (2000) used to deduce the absolute magnitudes of eight SNe Ia listed in Table 1 rely mainly on previous analysis of cepheids by Saha et al. (1994–1999). In our analysis, the cepheid distances re-analyzed by Gibson et al. (2000) have also been included to give a more appropriate estimate via a Bayesian approach. The absolute magnitudes derived by Parodi et al. (2000) without the second parameter corrections are  $0.05 \pm 0.08 \text{ mag}$  in  $B$ ,  $0.05 \pm 0.08 \text{ mag}$  in  $V$ ,  $0.09 \pm 0.12 \text{ mag}$  in  $I$  brighter than the counterparts we obtained. On the other hand, the second-parameter corrections will also influence the deduced absolute magnitudes. Despite the color-correction having nil effect on the deduced absolute magnitudes, as is shown in Eqs. (5)–(7), the luminosity dependence of SNe Ia on  $\Delta m_{15}(B)$  is found to be stronger than what Parodi et al. (2000) claimed (i.e.,  $0.60 \pm 0.10$  vs.  $0.44 \pm 0.13$  in  $B$ ). The discrepancy of the absolute magnitudes used for calibration increases to  $0.08 - 0.10 \text{ mag}$  after the second-parameter corrections. Had the absolute magnitudes in Eqs. (8)–(10) been tied to the zero-points in Figure 8 of Parodi et al. (2000), the mean value of  $H_0$  in  $B, V, I$  would have been  $63.2 \pm 2.0$  without considering any systematic errors. This result is in statistical agreement with Eq. (13).

A higher value of  $H_0 = 68 \pm 2 (\text{random}) \text{ km s}^{-1} \text{ Mpc}^{-1}$  was derived by Gibson et al. (2000). The absolute magnitudes they took are similar to ours, which are  $M_B = -19.51 \pm 0.06$  and  $M_V = -19.46 \pm 0.05$  without the  $\Delta m_{15}(B)$  correction, whereas they corrected the peak luminosity of SNe Ia based on the so-called reddening-free  $M_{B,V,I} - \Delta m_{15}(B)$  relation described by Phillips et al. (1999) and Suntzeff et al. (1999). As pointed out by Parodi et al. (2000), their higher order fit to  $\Delta m_{15}(B)$  may have introduced an over-correction, making the calibrators with small  $\langle \Delta m_{15}(B) \rangle$  too faint compared to the distant SNe Ia with larger  $\Delta m_{15}(B)$ . The formula introduced by Phillips et al. (1999) and Suntzeff et al. (1999) seems to be unsuitable to derive

a global luminosity correction for SNe Ia. Were the absolute magnitudes matched only to SNe Ia in spirals (usually slow decliners), both after Suntzeff's  $\Delta m_{15}(B)$  corrections, the value of  $H_0$  would be  $62.5 \text{ km s}^{-1} \text{ Mpc}^{-1}$ . Such a value is not in contradiction with our present result when the difference introduced by second-parameter corrections is considered.

There are many papers dealing with the determinations of  $H_0$  by means of SNe Ia (see Branch 1998 for a review). These measurements span a range from 55 to 68 in units of  $\text{km s}^{-1} \text{ Mpc}^{-1}$ . The differences are mainly caused by the absolute magnitudes used for calibration and the empirical relations used for luminosity correction. Generally speaking, the data of SNe Ia do not support a short distance scale.

## 6 THE VARIATIONS OF $H_0$ WITH DISTANCES

The fluctuation of the density will change the Hubble expansion by  $\delta H/H_0 = -\delta\rho/3\rho$ . The scatter in their peak luminosity being so remarkably small, the SNe Ia are an excellent means

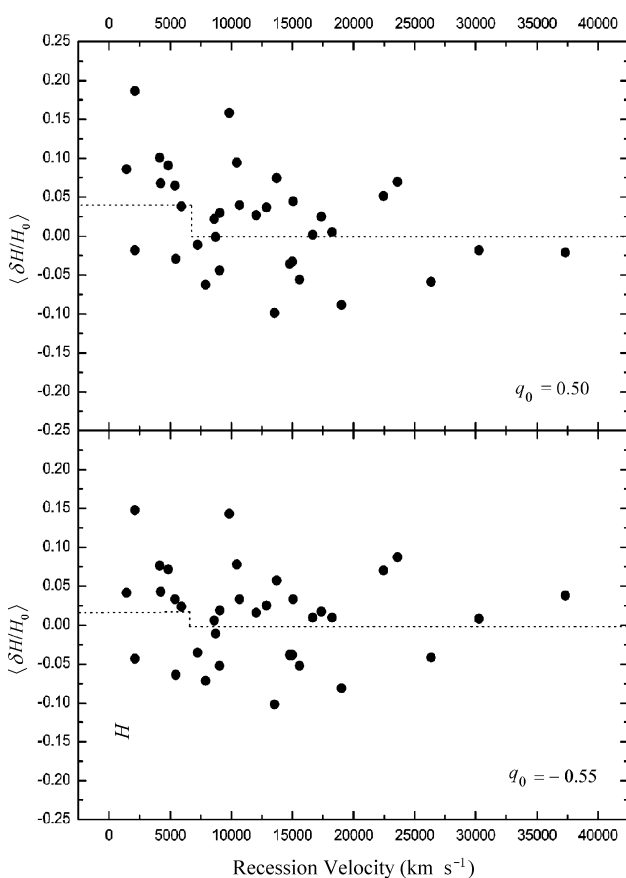


Fig. 6 The variations of  $H_0$  with redshift derived from the fiducial sample corrected for  $\Delta m_{15}(B)$  and  $(B_{\max} - V_{\max})$ .

for investigating the issue if the global value of  $H_0$  differs from the local value. Zehavi et al. (1998) claimed that an outward flow of 6.5% was found from data of 44 SNe Ia. The distances of SNe Ia they used were inferred by the method of multicolor light-curve shapes (MLCSs) (Riess et al. 1995). However, the absolute magnitude-light curve shape relation is not yet calibrated exactly, as is shown by the differences among recent works (Riess et al. 1995, 1998).

We use the fiducial sample of SNe Ia (which covers most of the data used in Zehavi et al. 1998), corrected for the parameters of  $\Delta m_{15}(B)$  and  $(B_{\max} - V_{\max})$ , to investigate the variation of  $H_0$  with distance. The variation of  $H_0$  is  $\delta H/H_0 = (H_i - H_0)/H_0$ , where  $H_i$  is the Hubble constant derived from the  $i$ -th SN Ia of the fiducial sample. We plot  $\delta H/H_0$  against redshift in Figure 6. Inspection of Figure 6 suggests a slight decrease of the Hubble constant from  $1400 \text{ km s}^{-1}$  to about  $20000 \text{ km s}^{-1}$  with  $q_0 = 0.50$ ; however, such a trend almost disappears with  $q_0 = -0.55$ . Following Zehavi et al. (1998), we divide the sample of SNe Ia into two zones divided at  $7000 \text{ km s}^{-1}$ . The statistical value

of  $H_0$  within  $7000 \text{ km s}^{-1}$  is marginally larger than that outside it by  $2.2 \pm 4.4\%$ . Even for a positive value of  $q_0$  (i.e.,  $q_0 = 0.50$ ), the excess is only  $4.0 \pm 4.5\%$ . Our results do not support an obvious local void. However, these results may be affected by the small size of the statistical sample, more data are needed to check them.

## 7 CONCLUSIONS

Blue SNe Ia are verified to be good distance indicators. The scatter in the raw Hubble diagram of the 35 fiducial sample of SNe Ia approaches  $\sim 0.20 \text{ mag}$ . The SNe Ia in early type galaxies tend to be systematically fainter than those in late type ones by  $0.16 - 0.19 \text{ mag}$ . The peak luminosities of SNe Ia are derived from eight nearby SNe Ia calibrators based on cepheid distances. They are estimated to  $19.50 \pm 0.08 \text{ mag}$  in  $B$ ,  $19.48 \pm 0.08 \text{ mag}$  in  $V$  and  $19.16 \pm 0.12 \text{ mag}$  in  $I$ . Direct match of these values to the Hubble-flow SNe Ia will underestimate the value of  $H_0$  because the former are derived from SNe Ia in spirals alone while the latter consist of SNe Ia in galaxies of different Hubble types.

On the other hand, the peak luminosities of SNe Ia are found to correlate with the parameters of decline rate  $\Delta m_{15}(B)$  and color ( $B_{\text{max}} - V_{\text{max}}$ ). If the Hubble-flow SNe Ia are corrected for these two parameters, the scatter in the Hubble diagram decreases to  $0.13 \text{ mag}$ , making the SNe the best distance indicator at present. When the peak luminosities of the calibrators after the corrections are matched to the corrected fiducial sample of SNe Ia, the value of  $H_0 = 63.6 \pm 1.8$  (random)  $\pm 5.7$  (systematic)  $\text{km s}^{-1} \text{ Mpc}^{-1}$  is obtained. The value  $H_0$  may be affected by the effect of metallicity on the cepheid distances and the uncertain value of  $q_0$ , both decreasing the value by  $2\% - 3\%$  when considered.

The variation of  $H_0$  with distance has been investigated with the corrected fiducial sample of SNe Ia. No obvious difference was found between the values determined from SNe Ia within and beyond  $7000 \text{ km s}^{-1}$  for an accelerating expansion universe ( $q_0 = -0.55$ ). For the Einstein-de Sitter universe ( $q_0 = 0.50$ ), the difference is marginal at  $4.0 \pm 4.5\%$ .

A better determination of the value of  $H_0$  needs our comprehensive understanding of the systematic errors discussed in Section 5. Besides, more sophisticated SNe Ia data with redshifts up to  $\sim 30000 \text{ km s}^{-1}$  will also help to map the variation of  $H_0$  with distance.

**Acknowledgements** Supported by the National Natural Science Foundation of China (19733002) and Project of "973" (G19990750401).

## References

- Alibert et al., 1999, A&A, 344, 551
- Beaulieu J. P. et al., 1997, A&A, 318, L47
- Blakeslee J. P., Tonry J. L., 1996, ApJ, 465, L19
- Bono G., Marconi M., Stellingwerf R. F., 1998, ApJS, 122, 167
- Branch D., Fisher A., Nugent P., 1993, AJ, 106, 2383
- Branch D., Romanishin W., Baron E. 1996, ApJ, 465, 73
- Branch D., 1998, ARA&A, 36, 17
- Feast W. W., 1999, PASP, 111, 775
- Ferderspiel M., Tammann G. A., Sandage A., 1998, ApJ, 495, 115
- Freedman W. L. et al., 2001, ApJ, in press
- Gibson B. K. et al., 2000, ApJ, 529, 628
- Hamuy M., Phillips M. M., Wells L. A., 1993, PASP, 105, 787

- Hamuy M. et al., 1996a, AJ, 112, 2398  
Hamuy M. et al., 1996b, AJ, 112, 2391  
Hoflich P. H., Khokhlov A. 1996, ApJ, 457, 500  
Hoflich P. et al., 1996, ApJ, 472, L81  
Jha et al., 1999, ApJS, 125, 73  
Kennicutt R. C. et al., 1998, ApJ, 498, 181  
Khokhlov A., Muller E., Hoflich P., 1993, A&A, 270, 223  
Kowal C. T. 1968, AJ, 73, 1021  
Lira P. et al., 1998, AJ, 115, 234  
Madore B. F., Freedman W. L. 1991, PASP, 103, 933  
Mazalli P. A. et al., 2000, astro-ph/0009490  
Parodi B. R. et al., ApJ, 2000, 540, 634  
Perlmutter S. 1997, ApJ, 483, 565  
Perlmutter S. et al., 1999, ApJ, 517, 565  
Phillips M. M., 1993, ApJ, 413, L105  
Phillips M. M., Lira P., Suntzeff N. B. et al., 1999, AJ, 118, 1766  
Pierce M. J., Jacoby G. H. 1995, AJ, 110, 2885  
Press W. H., In: J. N. Bahcall, J. P. Ostriker eds., *Unsolved Problems in Astrophysics* Princeton University Press, 1997  
Richtler T., Drenkhahn G., astro-ph/9909117  
Riess A. G., Press W. H., Kirshner R. P., 1995, ApJ, 438, L17  
Riess A. G., Press W. H., Kirshner R. P., 1996, ApJ, 473, 388  
Riess A. G. et al., 1998, AJ, 116, 1009  
Saha A. et al., 1994, ApJ, 425, 14  
Saha A. et al., 1995, ApJ, 438, 8  
Saha A. et al., 1996a, ApJ, 466, 55  
Saha A. et al., 1996b, ApJS, 107, 693  
Saha A. et al., 1997, ApJ, 486, 1  
Saha A. et al., 1999, ApJ, 522, 802  
Saha A., Labhardt L., Prosser Ch., 2000, PASP, 112, 163  
Sandage A., Bell R. A., Tripicco M. J., 1998, ApJ, 522, 250  
Sasselov D. et al., 1997, A&A, 324, 471  
Schaefer B. E., 1996, AJ, 111, 1668  
Schaefer B. E., 1996, ApJ, 460, L19  
Schaefer B. E., 1998, ApJ, 509, 80  
Schlegel D., Finkbeiner D., Davis M., 1998, ApJ, 500, 525  
Suntzeff N. B. et al., 1999, AJ, 117, 1175  
Tammann G. A., Sandage A., Saha A., astro-ph/0010422, In: M. Livio, K. Noll, M. Stiavelli, eds., *A Decade of HST Science*, Cambridge: Cambridge University Press  
Tanvir N. R. et al., 1995, Nature, 377, 27  
Tripp R., Branch D., 1999, ApJ, 525, 209  
Turner A. et al., 1998, ApJ, 525, 207  
Vaughan T. E. et al., 1995, ApJ, 439, 558  
Walker A. R. 1999, In: A. Heck, F. Caputo, eds., *Post-Hipparcos Cosmic Candles*, Dordrecht: Kluwer, p.125  
Wang L, Hoglich P., Wheeler J. C., 1997, ApJ, 483, L29  
Wells L. A. et al., 1994, AJ, 108, 2233  
Zehavi I. et al., 1998, ApJ, 503, 483